Nanotechnology Perceptions
ISSN 1660-6795
www.nano-ntp.com

Composite Ensemble Learning Model for Skin Cancer Detection from Dermatoscopic Images

Supriya L P[1], Rashmita Khilar[2]

[1]Department of Computer Science and Engineering, Saveetha School of Engineering, Saveetha Institute of Medical and Technical Sciences, Saveetha University, India
[2]Department of Information Technology, Saveetha School of Engineering, Saveetha Institute of Medical and Technical Sciences, Saveetha University, India
Email: supriyabinnyb@gmail.com

It is challenging to identify skin cancer using dermatoscopic scans because of their similar appearance and lack of color variation. Very less works have been developed on this dataset. Pre-processing processes such as hair removal, color improvement, segmentation, and noise removal are common in most of the approaches. These stages before classification complicate the models in terms of computing time. Dataset imbalance has not been focused on in most of the works that are considered in this work for performance improvement. Target-specific Augmentation is proposed to remove the data imbalance issue of the HAM10000 dataset that is publicly available on Kaggle. A new form of ensemble learning model named Composite Ensemble Learning (CEL) is proposed in this work by combining both homogeneous and heterogeneous models. The homogeneous part consists of two convolutional neural network (CNN) models. They are, nonetheless, trained through different input dataset patterns. One utilizes a direct dataset for training, whereas the other uses an increased level, balanced dataset. The long short-term memory (LSTM) model, whose learning mechanism is different from CNN's, is implemented for enhancing heterogeneity. A multilayer perceptron is implemented for the final classification (MLP). 98.6% accuracy is obtained by the proposed method which proved to be an improved performance in skin cancer detection.

Keywords: Dermatoscopic images, Skin Cancer Detection, Ensemble Learning, Convolutional Neural Network, Long Short-Term Memory, Data Augmentation.

1. Introduction

Cancer-promoting genetic alterations can be inherited from parents. Genetic mutations can also be obtained over one's lifespan as either a consequence of cell division mistakes or by coming in contact with radiation, like how the sun's UV radiation can cause skin cancer [1] [2]. Skin cancer can be divided into seven different types i.e. melanocytic nevi (Nv), melanoma (Mel), benign keratosis-like lesions (Bkl), basal cell carcinoma (Bcc),

actinic keratoses (Akiec), vascular lesions (Vasc), and dermatofibroma (Df). According to the survey report presented in [3], the expected number of new instances of melanoma skin cancer in 2020 was 324635, with 57043 persons dying that year. Early diagnosis followed by proper treatment will reduce this count. Because of the uneven forms and variable appearance of skin lesions, clinical manual screening of dermatoscopic or biopsy is time-consuming and difficult. Current-age technology like machine learning is progressing to overcome the time-consuming traditional methods.

Dermatoscopic images have been used to identify skin cancer in a variety of ways. Preprocessing methods are prioritized in the majority of tasks. Furthermore, classifying models contributes significantly to cancer detection. Authors in [4] have discussed many processes involved in several cutting-edge approaches. According to that study, several measures have been taken for skin cancer identification using dermatoscopic images. The essential processes in the diagnosis of dermal cancer include hair removal and a decline in noise, subdivision of the region affected from the entire picture, features extraction, selection, optimization, training, normalization of images, and classification. ABCD (Asymmetry, Border, Color, and Diameter) features [5] [6] [7] and Gray Level Co-Occurrence Matrix (GLCM) features [8] [9] have been frequently considered in skin cancer detection. Feature extraction step has a crucial role when considering statistical machine learning models e.g. Support vector machine (SVM), K-nearest neighbor (KNN), and random forest (RF) [10]. Whereas, deep learning models do not require any preprocessing steps and feature extraction steps as these models are capable of auto feature extraction. All of these preconceptions may be addressed with proper conjunction and selection of models, increasing accuracy of determining.

The collaborative learning technique has proved to be a well-performing method of training in computer vision. As an alternative to using a single model for training and classification, in ensemble learning, more than one classifier is used for parallel training. The final decision is taken by using either bagging, boosting, or stacking. Bagging simply averages the outputs of base classifiers trained in parallel to predict the final result. In boosting, the base classifiers follow sequential training instead of parallel which may lead to an expensive and time-consuming model. Stacking is somehow different from the two other methods and proved to be a better one. Stacking follows the training of another model concatenated to the parallel combination of base classifiers. Application of stacked ensemble learning includes brain tumor detection [11] [12], breast cancer detection [13] [14] [15], and many more. In this work, a new way of analyzing ensemble learning techniques is proposed for skin cancer detection. The highlights of exsisting work is summarized below:

- A target-specific Augmentation (T-Aug) model is designed to overcome the class imbalance problem of the dataset.
- Composite ensemble learning a model that combines homogeneous and heterogeneous elements is created using two CNNs and one LSTM as base classifiers.
- Looking into the size of predictions of base classifiers, a simple neural network i.e. the MLP is used to reduce the system complexity

This is the sequence in which the remainder of the paper is organized. Recent developments

in skin cancer detection are discussed in Section 2. Section 3 is prepared to describe the proposed method in detail. Results attained by the proposed method utilizing the given model are given and discussed in Section 4. This work is concluded and future scope is given in Section 5.

2. Literature Survey

Different techniques have been proposed in the field of skin cancer detection from dermatoscopic images. Data augmentation has been applied to the MED-NODE dataset [16] before training by deep learning models and it was found that it helped in increasing the system functionality. AlexNet, Google InceptionV3, and GoogleNet models are considered for confirmation purposes out of which AlexNet outperformed other models and provided maximum accuracy of 94% using enhanced data and 91% with no enhancement. The ensemble learning approach, has been adopted in [17] for skin cancer detection from HAM10000 dataset. The ensemble was formed using CNN models trained with the various kinds of input images that have been time-shifted. Skin dermatoscopic images have been studied using a region of interest-based deep learning model with transfer learning [18]. The ROI images were generated using a modified k-means algorithm. A hybrid architecture using the concept of transfer learning made a suggestion for cloud-based data backup in detecting melanoma [19]. This work was designed with various pre-processing and post-processing phases. Artifact removal and melanoma segmentation were considered pre-processing steps, whereas clinical feature extraction and quality of images enhancement were used for post-processing. A proposed method for the detection of skin lesions from dermatoscopic pictures involves two stages: segmentation and classification [20]. An encoder-decoder FCN model was used for segmentation and feature extraction followed by FCN-based DenseNet for classification. An ensemble model which is designed with a K-nearest neighbor and SVM with a linear and Gaussian kernels has been used [21]. In order to train the ensemble model, fractal signature features such as energy, variance, and entropy were assessed in addition to the deep features using Densenet-201.

A CNN model based on progressive learning [22] has been considered for classifying skin lesion. This model was trained with the synthetic data generated using GAN. The progressive nature has been established by utilizing two dissimilar datasets and then applying transfer learning for the test case. An encoder-decoder model has been used for hair removal from dermatoscopic images [23]. A mobile Android application was designed for skin lesion detection that was studied with 11 different CNN models [24]. Out of all the deep models used in that work, DenseNet-169 provided 92.25% highest accuracy to classify 7 classes of the HAM10000 dataset. Feature optimization has been utilized as a performance enhancer in [25], whereas the final classification was done using MLP. After going through different pre-processing steps, the authors used kernel fuzzy C-means for the segmentation of the desired lesions. Red fox optimization-based MLP was used for classification which was trained with selected features. Image augmentation plays a dynamic role in increasing the size of dataset. That method has been adopted in [26] along with mini-batch logic for class balance. The augmented and balanced dataset was used to train transfer learning-based CNN model. ABCD rule has been used as the detecting tool for skin cancer from dermatoscopic images [27]. The

images have gone through different pre-processing images such as noise removal and image enhancement using median filtering and contrast stretching. Also, the authors have used segmentation of skin lesion from whole image using thresholding. LabVIEW was used to implement each of these processes, and remarkable outcomes were obtained. Skin lesion localization, training, and classification have been adopted in [28] for skin cancer detection. That model is developed with two steps including localization using CNN along with high dimension contrast transform (HDCT) and feature extraction using DenseNet201 followed by t-distribution stochastic neighbor embedding (t-SNE). Then reduced features were used to train a multi-class ELM classifier that provided the final classification. A deep learning model that is cloud-based has been created to the HAM10000 dataset classification [29]. The authors in that work have used a CNN model stored in a cloud for automatic detection. An ensemble of five different classifiers trained with five different features such as local binary patterns, color HOGs, ABCD features, and deep features have been used for melanoma detection [30]. The final classification was done by the perceptron-based convolutional classifier in that work. Using various kinds of machine learning techniques, skin cancer detection pre-processing steps has been proposed [19]. In that work, the authors have applied dull razor method to remove hairs from the dermatoscopic images and a Gaussian filter for smoothing. A median filter was used for noise removal and edge detection of the lesion. K-means clustering was also applied for color-based segmentation. ABCD and GLCM features were then extracted for training and classification by the support vector machine model. In another work [32], an ensemble structure has been designed with CNN and multilayer perceptron models trained with direct images and statistical features respectively. The final classification was done by another MLP that was trained with the outcomes of base models. The final classifier could have been trained with the input images to observe the performance variation, however, it was not done in that work.

From the literature, it's observed that ensemble learning is not properly verified from all aspects. Improvement is still required, for this purpose a composite structure of the ensemble model is proposed for skin lesion classification with improved performance.

3. Proposed Methodology

Performance-wise, ensemble learning-based models perform better than single models.. This methodology, coupled with the class balancing method, is being evaluated for skin cancer diagnosis. Three base models and a single meta classifier comprise the ensemble model. Ensemble learning-based models are widely categorized into two types: heterogeneous and homogenous. Heterogeneous models use distinct basis classifiers, whereas homogeneous models use the base classifiers with the same learning algorithm [33]. In this work, we have considered the composition of homogeneous and homogeneous types of ensemble learning methods using two CNNs and one LSTM . One CNN model is trained using unbalanced dataset, while the other CNN model is trained using the balanced dataset. The same balanced dataset is also used to train the LSTM model. A MLP layer is added which provides the final decision. Final block diagram of the projected system is shown in Figure 1.

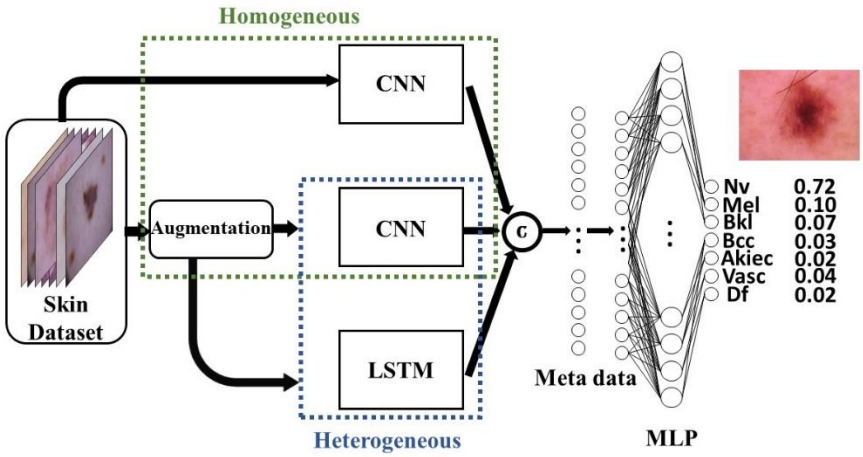

Figure 1. A Block diagram of the proposed model with sample image and prediction

3.1 Dataset Description

The study makes use of HAM10000 dataset, which is publicly available on Kaggle [34]. This dataset consists a total of 10015 dermatoscopic images from seven different classes of skin cancers such as melanocytic nevi (Nv), melanoma (Mel), benign keratosis-like lesions (Bkl), basal cell carcinoma (Bcc), actinic keratoses (Akiec), vascular lesions (Vasc), and dermatofibroma (Df), with 6705,1113, 1099,514,327,142 and 115 number of samples respectively. Each image has three channels since we only examined 28x28 RGB images. A ratio of 80:20 is used to divide the total dataset into train and test sets, yielding 8012 and 2003 samples in each set. Samples of each kind, skin cancer are shown in Figure 2.

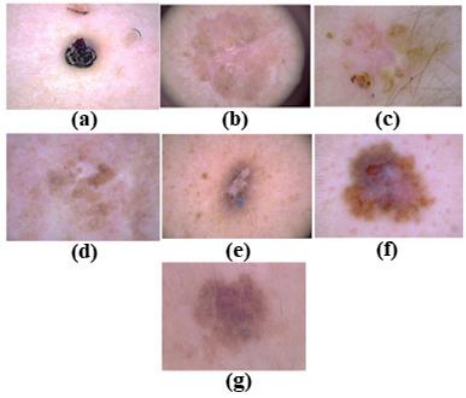

Figure 2. Sample dataset images (a) Vascular lesions, (b) Actinic Keratoses, (c)Basal cell carcinoma, (d) Benign keratosis-like lesions, (e) Dermatofibroma, (f) Melanoma, (g) Melanocytic nevi

3.2 Target-specific Augmentation

There is an enormous difference in the amount of images between the classes. This variation

might result in incorrect machine learning model training. Data augmentation is therefore done for each class that contains fewer images than the class with the greatest count in the train set while leaving the test set intact post-separation. The number of images of classes Mel, Bkl, Bcc, Akiec, Vasc, and Df are changed to 5378 each by applying data augmentation to match the data count of the class Nv.

Images are moved horizontally and vertically, flipped horizontally and vertically, and rotated at various angles, including 30, 45, 60, and 90 degrees, to balance the data. Other data augmentation techniques, such as brightness variation, are used between 0.2 and 0.9 to prevent data loss, and zooming is also performed on images between [0.5,1.0]. Algorithm 1 provides the augmentation procedures used to develop the target-specific augmentation (T-Aug) model.

The augmented train set, which contains a total of 37646 images with 5378 images in each class, is the result of the data augmentation. In the result section, a comparison of the impact of augmentation on training and training using direct data is shown.

Algorithm 1: Designing Target-based Augmentation

1. Input: Dataset $D = \{x_j, y_j\}_{j=1}^{m}$
2. Output: D_{aug}
3. Step 1: Access the data 'D'
4. Step 2: Class size evaluation
5. $n = \text{categorical}(y)$
6. $c = \text{counter}(n)$
7. $t = \max(c)$
8. Step 3: Import augmentation model (T-Aug)
9. For $j = 1$ to 6

a. $\text{Aug\_D}_j = \text{Aug}\ (D_j)$

b. If $\text{size}(\text{Aug\_D}_j) = t$

c. then Stop

10. End For
11. D_{aug} = Merge($\text{Aug\_D}_j, D_0$)

3.3 Stacked Ensemble Model Design

3.3.1 Convolutional Neural Network (CNN)

As CNNs have proved to be a better choice in image processing, in this work CNN models are chosen to design the proposed ensemble learning model. Two CNN models are used to learn the hyperparameters from the image datasets. The structure of each layer of CNN model is given in Table 1 for seven-class classification.

Table 1. Parameters of proposed CNN architecture

Layer (type)	Output Shape
Convolutional (2-D)	(28x28, 32)
MaxPooling (2-D)	(14x14, 32)
Convolutional (2-D)	(14x14, 64)
MaxPooling (2-D)	(12x12, 64)
Flatten	3136
Dense	7

Each CNN model has a straightforward design with a total of six levels, including two convolutional layers. As a result, the system is more able to handle small amounts of data, and it is also less complex and takes less time to perform the work. After each convolutional layer, max-pooling layer with strides equal to 2 is used to decrease the features to half, with the prominent values remaining.

The output (y) of each layer with input data (x) in the CNN model is evaluated using Eq. (1).

$$y = f(x) = \sigma(W * x + b) \quad (1)$$

Where σ represents the activation function, W represents the weights and b represents the bias involved in training. Convolutional layers are triggered using the ReLU activation function, while the last dense layer is turned on by applying the SoftMax activation method. The error of each model calculated using Binary cross-entropy (BCE) represented in Eq. (2).

$$BCE(y_{real}, y_{pred}) = -\sum_{I=1}^{2} y_{real} \log y_{pred} \quad (2)$$

Where y_{real} and y_{pred} represent the real label and predicted labels, respectively.

The detailed architecture of CNN model is shown in Figure 3.

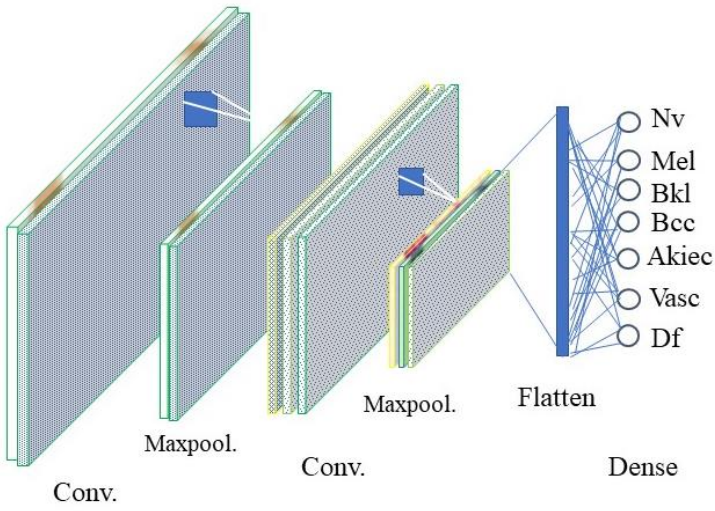

Figure 3. The architectural design of CNN model

3.3.2 Long Short-Term Memory (LSTM)

LSTM models have different training algorithms than CNNs, however, their performance in

handling images is also similar to CNNs [35]. The LSTM model is designed using two LSTM layers in hidden layer. A total of four layers are taken for designing the LSTM model. The first one is the input layer, and the next The final dense layer, which includes seven nodes for classification and is activated by the Softmax activation function, is made up of two layers with 32 and 64 LSTM layers respectively. The model is optimized for training using the Adam optimizer, and error function of the models is evaluated using the binary cross entropy loss function. Architecture of the designed LSTM model is shown in Figure 4.

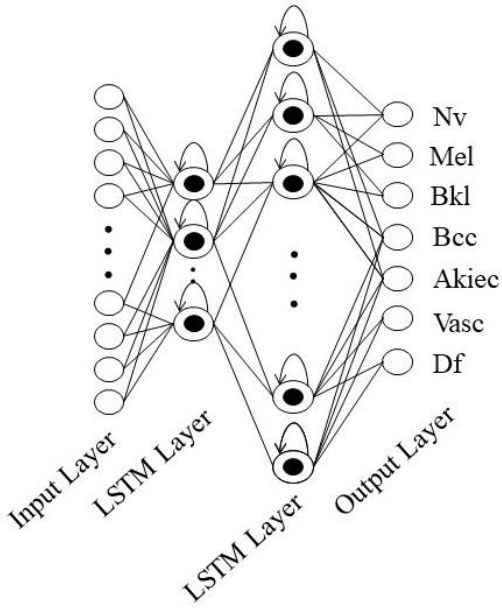

Figure 4. The architecture of designed LSTM model

The structure of LSTM model looks small, whereas it is sufficient to handle the input images of size 28x28 and also, it does not increase the system complexity.

3.3.3 MLP as meta classifier

The outputs of all first-stage classifiers are combined and transferred to a three-layered MLP for second-stage training and classification. The input data is received in the first layer, which is constructed with 21 nodes. In second layer SoftMax activation function is used to activate by the and the final layer is the dense. Finally the number of nodes in the final dense layer becomes 7 for seven class classifications. The training of MLP is provided in Algorithm 4.

Algorithm 4: Training of MLP

Input: Meta Data(MD) $=$ concatenate(Z_t, L_t)

Initialization

1. Load MLP

Training

2. No. of nodes in the output layer= no. of categorical labels (DS)

3. $y_{pred} = MLP(MD)$

Output: Class

Where Z_t stands for prediction probabilities and L_t for the matching labels predicted by CNNs.

4 Results and Discussion

4.1 Performance Evaluation

The unbalanced data is initially shown visually as in Figure 5. The class variance is so great that it may have an impact on how the classifying models are trained.

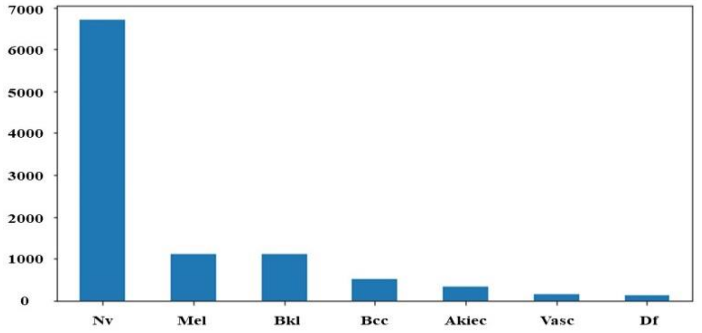

Figure 5. Bar plot showing data imbalance in the dataset

The training set created by taking into account 80% of entire dataset and for the class of Nv, 5378 images are found to be, highest number. T-Aug model is used to solve the class imbalance issue, resulting in 5378 images for each class. In Figure 6, the balanced class is depicted. Figure 7 displays the results of several augmentation sub-strategies for a sample input picture.

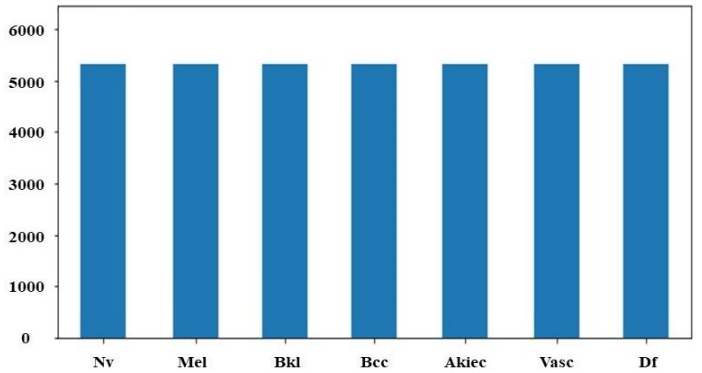

Figure 6. Bar plot showing the balanced dataset

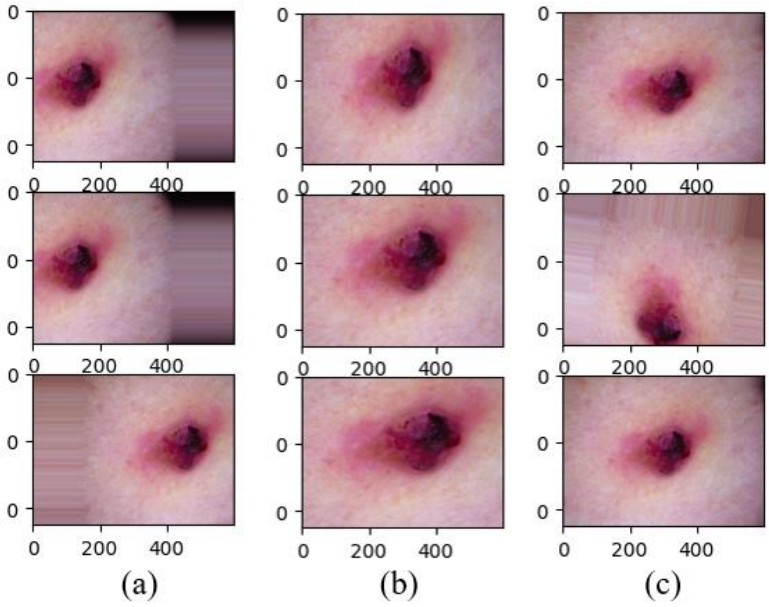

Figure 7. Outputs after applying (a) horizontal shift, (b) zoom, (c) random shift

Table 2 lists the training, validation and testing results of each set of data and the models. CNNs and LSTM are verified with both unbalanced and balanced datasets to check the effects of data balancing on the models.

Table 2. Performance metrics of each model with different forms of dataset

		Training Accuracy (in %)	Validation Accuracy (in %)	Testing Accuracy (in %)
Direct Data	CNN	87.92	86.03	81.39
	LSTM	87.02	85.41	80.81
Balanced Data	CNN	94.01	91.01	88.39
	LSTM	93.19	89.61	87.47

Table 2 shows that class imbalance negatively influences model performance, but a balanced dataset improves the accuracy of deep learning model training compared to unbalanced data. Figure 8 shows the testing accuracy from both the composite model and the individual model.

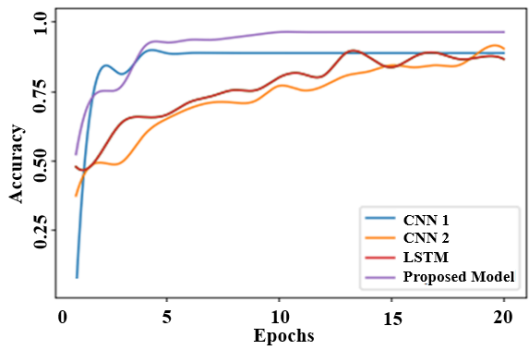

Figure 8. Accuracy comparison between base classifiers and proposed composite model

Using the previously produced test set, the performance of each base model and the suggested one is also evaluated. The results that were discovered at this point are shown in terms of confusion matrix in Figure 9. The suggested composite model has the best test accuracy of 98.6%.

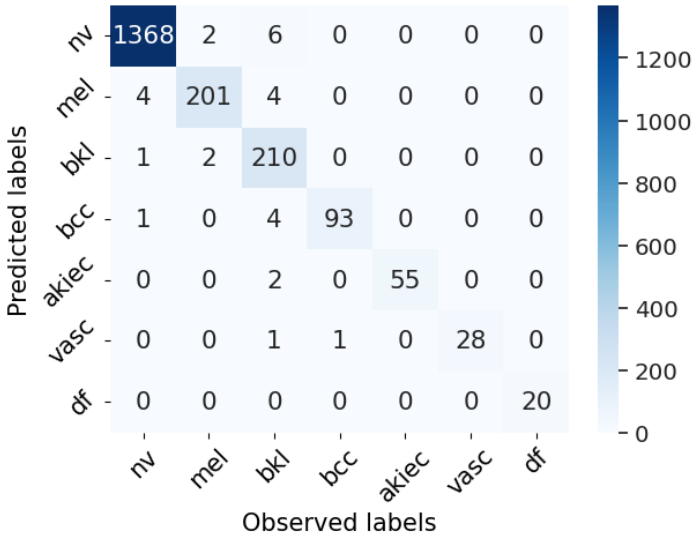

Figure 9. Confusion matrix of proposed composite ensemble model.

Starting with test data from the original dataset's 2003 numbers, confusion matrices are produced in Figure 9. The same set applies to all models. The accuracy, F1 score, precision, and recall of suggested model are calculated using confusion matrix. The best testing accuracy is demonstrated by the suggested composite ensemble model. Using Eqn. (3-6), the accuracy and other factors were assessed.

$$\text{Accuracy} = \frac{\text{TP+TN}}{\text{TP+TN+FP+FN}} \times 100 \quad (3)$$

$$\text{Precision} = \frac{\text{TP}}{\text{TP+FP}} \times 100 \quad (4)$$

$$\text{Recall} = \frac{\text{TP}}{\text{TP+FN}} \times 100 \quad (5)$$

$$\text{F1 Score} = 2 \times \frac{\text{Recall} \times \text{Precision}}{\text{Recall+Precision}} \quad (6)$$

The suggested composite ensemble model is compared to the state-of-art models in Table 3.

Table 3. Comparison of the proposed composite ensemble model with the state-of-art models

Reference	Pre-processing	Feature extraction	Classification	Testing Accuracy (in %)
[16]	Image resize, zero normalization, and augmentation	FPN and RPN	Ensemble of three CNN	81.3
[17]	Time-shifted forms of input images	-	Ensemble of CNN	83.8
[19]	Localization using CNN	DenseNet201	ELM	88.39

[20]	Augmentation	-	Transfer learning-based CNN	89.97
[22]	-	GAN	Progressive learning-based CNN	92.3
[23]	Noise removal using Type II fuzzy	FSPO	Deep Q Net	92.364
[24]	Augmentation, Artifact removal, melanoma segmentation, image quality enhancement	Clinical feature	AlexNet	94
[25]	-	Color features using LBP and Geometrical features	Ensemble of ML models	95.35
[26]	-	-	HMM	96
[27]	Hair removal, noise reduction, segmentation by cropping, and binarization	Textural, shape, and color feature	KNN, SVM, and Decision tree	96.68
[29]	ROI image generation	-	Transfer Learning DNN	97.2
[30]	-	LBP, color HOGs, ABCD, and deep features	Perceptron-based convolutional classifier	97.5
[31]	Hair removal and Segmentation	ABCD, GLCM, LBP	ANN	97.7
Proposed work	Target-Specific Augmentation	-	Ensemble of two CNNs, one LSTM as base models and MLP as meta classifier	98.6

4.2 Discussion

As shown in Table 2, class imbalance has a negative impact on the classifying models' training. Figures 5 and 6 compare the application of T-Aug, which proved to be a wise decision in this regard. However, the performance of the base classifiers is insufficient to match that of the earlier works. This provided motivation for researchers to employ ensemble learning techniques in novel ways. Combining both homogeneous and heterogeneous learning into a single model is known as the composite ensemble learning model. While comparing the base classifiers and state-of-the-art methods, its performance has been significantly enhanced. Figure 9 and Table 3 show this analysis as a confusion matrix and comparison table, respectively.

5 Conclusion

When used properly, ensemble learning-based models may compete with modern deep learning models with intricate and lengthy architecture. With the right use of a greatly enhanced ensemble learning approach, this observation is shown to be accurate. This study supports this theory and offers a more accurate method for observing deep learning and ensemble learning variations. Target-specific augmentation for class balancing is used to verify the class imbalance issue and solve it. Analyzing classification issues with a composite ensemble model that includes homogeneous and heterogeneous combinations turned out to more effective and novel. A test accuracy of 98.6% was achieved using deep learning models

such as CNNs and LSTM in combined form, outperforming the leading models in the diagnosis of skin cancer field. The use of proposed composite ensemble learning method will be verified with different biomedical images in the future.

Declarations

Funding: The authors did not receive support from any organization for the submitted work.

Conflict of Interest: The authors declare that they have no conflict of interest.

Ethical approval: This article does not contain any studies with human participants or animals performed by any of the authors.

Informed Consent: This article does not contain patient data.

References

1. F. R. De Gruijl, "Skin cancer and solar UV radiation," European Journal of Cancer, vol. 35, p. 2003–2009, 1999.
2. O. Gefeller and K. Diehl, Children and ultraviolet radiation, Children, vol. 9(4), p. 537. 2022.
3. National Cancer Institute,Available from:https://www.cancer.gov/about-cancer/understanding/what-is-cancer.
4. M. Dildar, S. Akram, M. Irfan, H. U. Khan, M. Ramzan, A. R. Mahmood, S. A. Alsaiari, A. H. M. Saeed, M. O. Alraddadi and M. H. Mahnashi, "Skin cancer detection: a review using deep learning techniques," International journal of environmental research and public health, vol. 18, p. 5479, 2021.
5. G. Argenziano, G. Fabbrocini, P. Carli, V. De Giorgi, E. Sammarco and M. Delfino, "Epiluminescence microscopy for the diagnosis of doubtful melanocytic skin lesions: comparison of the ABCD rule of dermatoscopy and a new 7-point checklist based on pattern analysis," Archives of dermatology, vol. 134, p. 1563–1570, 1998.
6. D. N. H. Thanh, V. B. Prasath, L. M. Hieu and N. N. Hien, "Melanoma skin cancer detection method based on adaptive principal curvature, colour normalisation and feature extraction with the ABCD rule," Journal of Digital Imaging, vol. 33, p. 574–585, 2020.
7. Z. She, Y. Liu and A. Damatoa, "Combination of features from skin pattern and ABCD analysis for lesion classification," Skin Research and Technology, vol. 13, p. 25–33, 2007.
8. X. Ou, W. Pan and P. Xiao, "In vivo skin capacitive imaging analysis by using grey level co-occurrence matrix (GLCM)," International journal of pharmaceutics, vol. 460, p. 28–32, 2014.
9. Z. Abbas, M.-u. Rehman, S. Najam and S. D. Rizvi, "An efficient gray-level co-occurrence matrix (GLCM) based approach towards classification of skin lesion," in 2019 amity international conference on artificial intelligence (AICAI), 2019.
10. A. Murugan, S. A. H. Nair and K. P. Kumar, "Detection of skin cancer using SVM, random forest and kNN classifiers," Journal of medical systems, vol. 43, p. 1–9, 2019.
11. A. Das, S. K. Mohapatra and M. N. Mohanty, "Design of deep ensemble classifier with fuzzy decision method for biomedical image classification," Applied Soft Computing, vol. 115, p. 108178, 2022.
12. M. M. Zahoor, S. A. Qureshi, S. Bibi, S. H. Khan, A. Khan, U. Ghafoor and M. R. Bhutta, "A New Deep Hybrid Boosted and Ensemble Learning-Based Brain Tumor Analysis Using MRI," Sensors, vol. 22, p. 2726, 2022.
13. A. Das, M. N. Mohanty, P. K. Mallick, P. Tiwari, K. Muhammad and H. Zhu, "Breast cancer detection using an ensemble deep learning method," Biomedical Signal Processing and

Control, vol. 70, p. 103009, 2021.
14. A. Das and M. N. Mohanty, "Design of ensemble recurrent model with stacked fuzzy ARTMAP for breast cancer detection," Applied Computing and Informatics, 2022.
15. R. Rasti, M. Teshnehlab and S. L. Phung, "Breast cancer diagnosis in DCE-MRI using mixture ensemble of convolutional neural networks," Pattern Recognition, vol. 72, p. 381–390, 2017.
16. I. Giotis, N. Molders, S. Land, M. Biehl, M. F. Jonkman and N. Petkov, "MED-NODE: A computer-assisted melanoma diagnosis system using non-dermoscopic images," Expert systems with applications, vol. 42, p. 6578–6585, 2015.
17. K. Thurnhofer-Hemsi, E. López-Rubio, E. Domínguez and D. A. Elizondo, "Skin lesion classification by ensembles of deep convolutional networks and regularly spaced shifting," IEEE Access, vol. 9, p. 112193–112205, 2021.
18. R. Ashraf, S. Afzal, A. U. Rehman, S. Gul, J. Baber, M. Bakhtyar, I. Mehmood, O.-Y. Song and M. Maqsood, "Region-of-interest based transfer learning assisted framework for skin cancer detection," IEEE Access, vol. 8, p. 147858–147871, 2020.
19. L. Di Biasi, A. A. Citarella, M. Risi and G. Tortora, "A Cloud Approach for Melanoma Detection Based on Deep Learning Networks," IEEE Journal of Biomedical and Health Informatics, vol. 26, p. 962–972, 2021.
20. A. A. Adegun and S. Viriri, "FCN-based DenseNet framework for automated detection and classification of skin lesions in dermoscopy images," IEEE Access, vol. 8, p. 150377–150396, 2020.
21. E. O. Molina-Molina, S. Solorza-Calderón and J. Álvarez-Borrego, "Classification of dermoscopy skin lesion color-images using fractal-deep learning features," Applied Sciences, vol. 10, p. 5954, 2020.
22. Y. Gu, Z. Ge, C. P. Bonnington and J. Zhou, "Progressive transfer learning and adversarial domain adaptation for cross-domain skin disease classification," IEEE journal of biomedical and health informatics, vol. 24, p. 1379–1393, 2019.
23. L. Talavera-Martinez, P. Bibiloni and M. Gonzalez-Hidalgo, "Hair segmentation and removal in dermoscopic images using deep learning," IEEE Access, vol. 9, p. 2694–2704, 2020.
24. I. Kousis, I. Perikos, I. Hatzilygeroudis and M. Virvou, "Deep Learning Methods for Accurate Skin Cancer Recognition and Mobile Application," Electronics, vol. 11, p. 1294, 2022.
25. Z. Fu, J. An, Q. Yang, H. Yuan, Y. Sun and H. Ebrahimian, "Skin cancer detection using Kernel Fuzzy C-means and Developed Red Fox Optimization algorithm," Biomedical Signal Processing and Control, vol. 71, p. 103160, 2022.
26. T.-C. Pham, A. Doucet, C.-M. Luong, C.-T. Tran and V.-D. Hoang, "Improving skin-disease classification based on customized loss function combined with balanced mini-batch logic and real-time image augmentation," IEEE Access, vol. 8, p. 150725–150737, 2020.
27. S. Saravanan, B. Heshma, A. A. Shanofer and R. Vanithamani, "Skin cancer detection using dermoscope images," Materials Today: Proceedings, vol. 33, p. 4823–4827, 2020.
28. M. A. Khan, K. Muhammad, M. Sharif, T. Akram and V. H. C. de Albuquerque, "Multi-class skin lesion detection and classification via teledermatology," IEEE Journal of Biomedical and Health Informatics, vol. 25, p. 4267–4275, 2021.
29. M. A. Kadampur and S. Al Riyaee, "Skin cancer detection: Applying a deep learning based model driven architecture in the cloud for classifying dermal cell images," Informatics in Medicine Unlocked, vol. 18, p. 100282, 2020.
30. L. Ichim and D. Popescu, "Melanoma detection using an objective system based on multiple connected neural networks," IEEE Access, vol. 8, p. 179189–179202, 2020.
31. M. K. Monika, N. A. Vignesh, C. U. Kumari, M. N. V. S. S. Kumar and E. L. Lydia, "Skin cancer detection and classification using machine learning," Materials Today: Proceedings, vol. 33, p. 4266–4270, 2020.
32. A. Das, S. K. Mohapatra and M. N. Mohanty, "A Concatenated Model with Deep Learning

Technique for Skin Lesion Detection," in 2021 5th International Conference on Information Systems and Computer Networks (ISCON), 2021.

33. A. Das, S. K. Mohapatra and M. N. Mohanty, "Brain Image Classification Using Optimized Extreme Gradient Boosting Ensemble Classifier," in Biologically Inspired Techniques in Many Criteria Decision Making: Proceedings of BITMDM 2021 (pp. 221-229). Singapore: Springer Nature Singapore. 2022.
34. P. Tschandl, C. Rosendahl and H. Kittler, "The HAM10000 dataset, a large collection of multi-source dermatoscopic images of common pigmented skin lesions," Scientific data, vol. 5, p. 1–9, 2018.
35. A. Das, G. R. Patra, & M. N. Mohanty. A comparison study of recurrent neural networks in recognition of handwritten Odia numerals. In International Conference on Emerging Trends and Advances in Electrical Engineering and Renewable Energy (pp. 251-260). Singapore: Springer Nature Singapore. 2020.